Transactions, SMiRT-24
BEXCO, Busan, Korea - August 20-25, 2017
Division SS

STUDY ON ESTIMATION OF THE FAULT MODEL OF KAMISHIRO EARTHQUAKE USING DYNAMIC FAULT RUPTURE SIMULATION

Yuta Mitsuhashi[1], Gaku Hashimoto[2], Hiroshi Okuda[3], Fujio Uchiyama[4] and Akari Yoshino[5]

[1] Senior Staff, KOZO KEIKAKU ENGINEERING Inc., Japan
[2] Lecturer, Graduate School of Frontier Sciences, The University of Tokyo, Japan
[3] Professor, Graduate School of Frontier Sciences, The University of Tokyo, Japan
[4] Manager, KOZO KEIKAKU ENGINEERING Inc., Japan
[5] KOZO KEIKAKU ENGINEERING Inc., Japan

ABSTRACT

In recent years, new demand has appeared for evaluations of earthquake fault displacement to address the need to evaluate the soundness of underground structures. Fault displacement is caused by the rupturing of earthquake source faults, and is investigated through the use of such methods as the finite difference method and the finite element method (FEM). We conducted dynamic rupture simulations on the Kamishiro Fault Earthquake using nonlinear FEM, focused on time history of fault displacement and response displacement, and demonstrated an ability to simulate observed values to a certain extent. During these simulations, we created models of homogeneous faults using the ground as the solid element and fault planes as joint elements. Although we were able to roughly simulate displacement time histories, obstacles to achieving more precise simulations still exist. In this research, we conducted investigations to model strong motion generation areas (SMGA). We conducted a searching analysis using Bayesian optimization with SMGA distribution within faults as parameters, and estimated the optimal parameters for simulating time histories of displacement. In addition, we compared our results with estimations of SMGA derived from different methods, and demonstrated that our distributions qualitatively matched. To conduct the simulation, we introduced joint elements from Goodman et al. that had been expanded to the FEM code FrontISTR, which makes it possible to analyze large-scale models.

INTRODUCTION

In Japan, there is a pressing need to clarify how fault displacement that occurs at nuclear power plant properties affects the facilities, and recent years have seen spirited debate on the matter in organizations such as the Atomic Energy Society of Japan's Investigation Committee on the Evaluation of Fault Activity and Industrial Risk, etc. Evaluations of fault displacement (Japan Nuclear Safety Institute On-site Fault Assessment Method Review Committee, 2014) are required to address the need to evaluate the soundness of critical underground structures and the like on nuclear power plant properties, but conducting these evaluations is difficult due to their stochasticity and rare examples. Fault displacement is caused by the rupturing of earthquake source faults, and has long been investigated through the use of finite difference methods (Dan el al. 2007, Irie et la. 2010) and FEM (Mizumoto et al. 2001, 2005). In particular, a great deal of research that focuses on finite difference methods has been conducted regarding dynamic simulations that use slip-weakening models to simulate the process of the spontaneous rupture of faults.

We used three-dimensional, nonlinear FEM to conduct a simulation of the Kamishiro Fault Earthquake (Mitsuhashi et al. 2016), which struck Nagano Prefecture on November 22, 2014, and demonstrated the ability to simulate observational data to a certain extent through an analysis that modeled a constant stress drop within fault planes. We created models of 40 km times 40 km times 20 km areas that included earthquake source faults, with the ground as the solid element and fault planes as joint elements.

We used nonlinear constitutive laws that incorporated stress drop to model the process of fault rupture, caused the fault rupture by applying initial stress to the joint element as an initial condition, and compared the response time histories of the ground surface that resulted from the propagation of the rupture to the observational data from K-net. In addition, we compared fault displacement at ground surface observed through field surveys after the earthquake to the displacement values we obtained through our analysis. We assumed that the stress drop of a fault is uniform throughout the fault plane. We were able to simulate observational data to a certain extent under the assumption of the uniform distribution of stress drop throughout the fault plane, but concluded that fault structures must be modeled in greater detail to achieve more precise results. In light of the above, we conducted this research using analyses that used more detailed fault models in an attempt to achieve more precise results.

We conducted this research using the FEM code FrontISTR (FrontISTR Workshop HP, 2017), which makes it possible to use parallel computing on large-scale models. This enabled us to use a relatively detailed mesh to analyze an expansive area of ground.

KAMISHIRO FAULT EAERTHQUAKE AND ITS SIMULATON

The Kamishiro Fault Earthquake was a reverse-fault earthquake whose earthquake source fault extended approximately 20 km along part of the Kamishiro Fault and to its north, and was approximately 10 km deep. The magnitude was 6.7, and the moment magnitude was 6.2. Fault displacement at the ground surface of up to roughly 1 m has been confirmed along a total length of 9 km (Japan Association for Earthquake Engineering 2015, National Research Institute for Earth Science and Disaster Prevention 2015, National Institute of Advanced Industrial Science and Technology 2015). In addition, acceleration of up to roughly 600 Gal was observed at the K-NET observation point near the fault.

One example of research on the Kamishiro Fault Earthquake is the fault model created by Ikeda et al. 2016, using the forward modeling method based on the empirical Green's function method. The empirical Green's function method is an analytical method in which a fault is divided into smaller faults, and the target earthquake is expressed as superposition of smaller earthquakes generated from those smaller faults. Ikeda et al. used aftershocks that occurred directly after the main shock to build a fault model that simulated observational data from the main shock. They set the size of earthquakes generated from the smaller faults as an indeterminate parameter, and searched for parameters that would enable them to simulate observational data. The empirical Green's function method enables researchers to express target earthquakes as linearized superposition of smaller earthquakes, thus enabling them to use the least squares method and other optimization methods to search for parameters that match observational data most closely (earthquake inversion analysis). Ikeda et al. pointed out that locating strong motion generation areas (SMGA) near hypocenters makes it possible to simulate observational data. SMGA are areas within faults that produce the most energy, and locating rectangular SMGA within faults simulate the heterogeneity of faults.

We used three-dimensional, nonlinear FEM to conduct dynamic simulations of the Kamishiro Fault Earthquake. The dynamic simulations modeled faults according to the relationship of nonlinear stress distortion. We used this method to simulate the process of fault rupturing. We did so by intentionally applying great initial stress to the hypocenter to cause the fault to slip and release stress, and to propagate that stress throughout the fault. We used the joint elements shown in Figure 1 to model the fault. Joint elements are finite elements that simplistically simulate contact, sliding and separation between two objects. Many joint elements have been devised, including those developed by Goodman 1976 and those formulated based on three-dimensional isoparametric elements. We expanded the Goodman joint elements into arbitrary shapes (Mitsuhashi et al. 2016). We set the stress drop to a uniform 1.0 MPa as the condition in which the moment magnitude Mw approached observed values from the actual earthquake. We calculated Mw with variance Δu of each element in the final state of the analysis in Equation (1) and Equation (2), with fault plane Σ. We determined τ_y using Equation (3), with Andrew 1976 as a reference.

$$M_0 = \int_{\Sigma} \mu \Delta u dS \quad (1)$$

$$Mw = \frac{1}{3}\log_{10} M_0 - 6.1 \quad (2)$$

$$\tau_y = 1.6\Delta\sigma \quad (3)$$

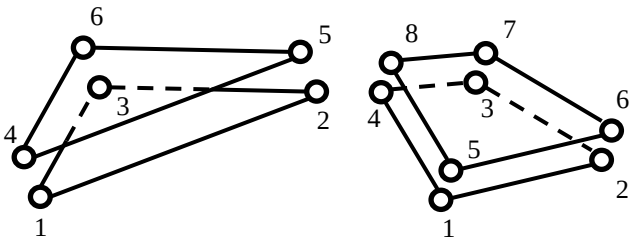

Figure 1. Joint Element

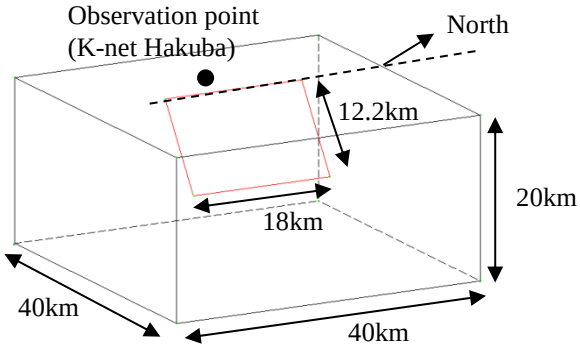

Figure 2. Analysis model

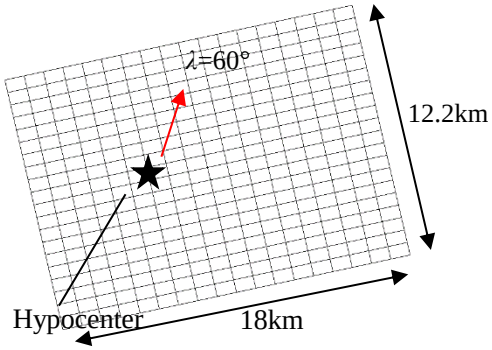

Figure 3. Analysis model of the fault

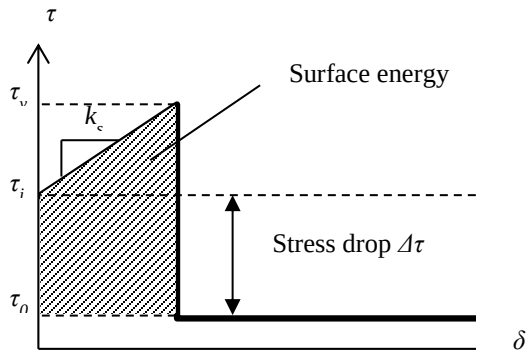

Figure 4. Stress displacement relation

Table 1. Fault parameter

Fault width	W	12.2	km
Fault length	L	18.0	km
Strike angle	θ	12	degree
Dip angle	δ	50	degree
Stress drop	$\Delta\tau$	1.00	MPa
Fault shearing stiffness	k_s	1.20×10^4	kN/m/m^2
Fault vertical stiffness	k_v	1.20×10^4	kN/m/m^2

We demonstrated an ability to simulate observational data to a certain extent by analyzing fault plane interiors modeled with uniform structures. Then we compared the response time histories of the ground surface that resulted from the propagation of the rupture to the observational data from K-net. In addition, we compared ground surface fault displacement observed through field surveys after the earthquake to the displacement values we obtained through our analysis. We were able to simulate

observational data to a certain extent under the assumption of the uniform structure of the fault plane, but concluded that fault structures must be modeled in detail to achieve more precise results.

SEARCH OF SMGA

Modeling SMGA

We conducted a dynamic simulation to model SMGA in an effort to conduct a dynamic simulation using a more complex fault model. We considered SMGA as areas that generated the largest amounts of energy within fault, and modeled SMGA by defining areas with high stress drop values. We assumed circular SMGA and set radius and center positions (in terms of the strike and the dip) as parameters, and searched for optimal parameters for simulating observational data. We set the radius of each search range from 0.0 km (the case that SMGA was not modeled) to 6.0 km, and the position of each search range as all points on each fault plane. We then divided each search range into 20 parts, and defined the resulting grids as search areas. As for search points, there were 9,261 patterns (2^{13}).

When we used the fault model with uniform properties, we set the stress drop, which we had previously set to a uniform 1.0 MPa, to 2.0 MPa in SMGA. However, doing so with the stress drop in background areas fixed at 1.0 MPa causes the seismic moment in faults to increase, and makes it impossible to compare individual cases. Thus, we decreased the stress drop in background areas so that the average stress drop would stay constant. When the SMGA radius was 1 km, the ratio between the stress drop in the SMGA and the stress drop in background areas was roughly 2.03; when the radius was 5 km, the ratio was roughly 4.51. It is worth noting that the analytical model from the authors' investigation is somewhat divergent from the "recipe" of Irikura et al. 2003; according to the recipe, the average asperity area for a typical inland earthquake is 22% of the total rupture area, and the stress drop of SMGA is roughly 4.5 times the average stress drop. This means that, when stress drop values in SMGA are high, larger SMGA result in negative values for stress drop in background areas. To avoid this issue, we intend to conduct analysis with stress drop as a parameter in the future.

Search Methodology

Approximately a few hour is required to analyze each case in these simulations; identifying the optimal case among the total of 9,261 cases for analysis would require a massive amount of computational resources. In addition, the only parameters for this investigation were the radius and positions of SMGA assumed to be circular; adding more parameters such as SMGA shapes and stress drop values would produce more cases, which would make a brute-force search unrealistic. Furthermore, in this investigation, we sought to use linear programming and the like to derive optimal solutions. As explained previously, the empirical Green's function method simulate conditions in linearized superposition of smaller earthquakes. In dynamic simulations, this method models fault slips according to nonlinear constitutive laws of the smaller faults; thus this method cannot express conditions in simple superposition of small earthquakes. Examples of inversion analysis used in dynamic rupture simulations include methods using the Monte Carlo Method described by Peyrat et al. 2004 and methods based on the Walsh functions described by Goto et al. 2006. In this research, we used Bayesian optimization as the method for searching for optimal locations.

Evaluating Degree of Adaptively

In this research, we conducted a search to find the smallest difference between the displacement time histories from observational data from the K-net Hakuba observation point, and from the results of FEM analysis. There are many approaches as to the definition of "difference." They include (a) the square root of the sum of squares, (b)maximum displacement, (c)maximum displacement during time histories, and (d)displacement at the final step. Given this, we simulated a random sample of 300 model cases from the search areas described previously, and calculated correlation coefficients for parameters of individual errors

in those analysis results. Table 2 shows these correlation coefficients. Each of the correlation coefficients regarding the absolute value of the time historical maximums is low, and the absolute values of all other correlation coefficients are high. In other words, the correlation coefficients regarding the absolute value of the time historical maximums cannot be used to evaluate the other error values, but any of the other correlation coefficients is sufficient to evaluate the other error values.

In light of these results, we defined error for the purposes of this investigation as the square root of the sum of squares. Three components can be derived from displacement time histories, but we decided to use only the Z-axis component, also due to sufficient correlativity. We defined the degree of adaptively as the inverse of the error, and conducted a search for the parameters with the highest degrees of adaptively.

Bayesian Optimization

Table 2. Correlation coefficients of each parameters

	(a)	(b)	(c)	(d)
(a)	-	-0.679	0.121	-0.742
(b)	-	-	-0.055	0.958
(c)	-	-	-	0.023
(d)	-	-	-	-

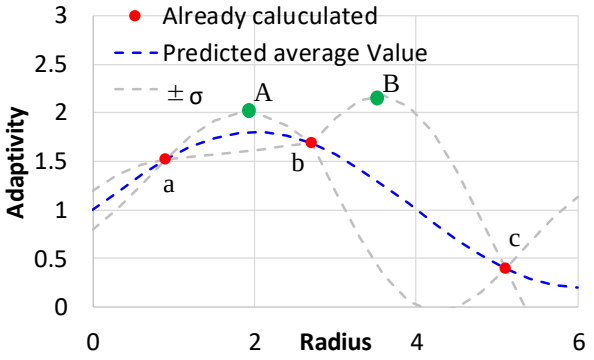

Figure 6. Image of Gaussian Process

Bayesian optimization is method of searching for parameters using a Gaussian Process (GP; Rasmussen et al. 2006). As a method of nonparametric expression that does not depend on distribution, we speculated Bayesian optimization could also be used to express the response of the results of highly nonlinear analysis. GP can use previous sample data to learn regression function models, and can predict output when supplied with new sample data. In other words, GP can use the results of sequential analysis to update prediction functions and immediately select samples for the ensuing analysis case with a higher degree of certainty.

Figure 6 is an image of GP with an SMGA radius as the only search parameter. Assuming that points a, b and c are points for which searches are complete, regression analysis using GP can be used to derive predicted average values and standard deviations for the entire search range. Looking only at predicted average values, Point A appears to be a candidate for the ensuing search. Conversely, the space between points b and c is wider than the space between points a and b, which means that the standard deviation between points b and c is evaluated as larger; when one standard deviation is taken into consideration, Point B appears to be a candidate for the ensuing search. This makes points with higher predicted degrees of adaptively more likely to be chosen, and decreases the number of points already searched, which makes points that may have a high degree of adaptively candidates for the ensuing search.

Search Results

In searches that use GP, multiple points must be provided as initial values. Thus, we decided to use as initial values the 300 cases used in the correlativity analysis described previously. We used a supercomputer to conduct this analysis; this considerable computational resource enabled us to analyze multiple cases in the same time. In contrast, GP methods can only determine one ensuing analytical model at a time from data sets that comprise currently complete analyses. Thus, we used the following procedure to create analytical models of 100 cases.

1. Use the results of currently complete analyses $\{(x_i, y_i), i=1\sim N\}$ to create Analytical Model A_{max} that corresponds to the maximum x-value x_{max} from $f(x_{max}) + \alpha\sigma(x_{max})$.
2. Suppose that the analysis results of A_{max} equal $f(x_{max})$. Let $\{(x_i, y_i), i=1\sim N\} \cup (x_{max}, f(x_{max}))$ equal cases for which analysis is complete, and create an analytical model that corresponds to the maximum x-value from $f(x_{max}) + \alpha\sigma(x_{max})$.
3. If the analytical models created previously include cases for which analysis is complete, let $\alpha = \alpha * 2$ and return to Step (2).
4. Repeat Step (2) until 100 model cases are created.
5. Conduct analyses on the 100 cases.

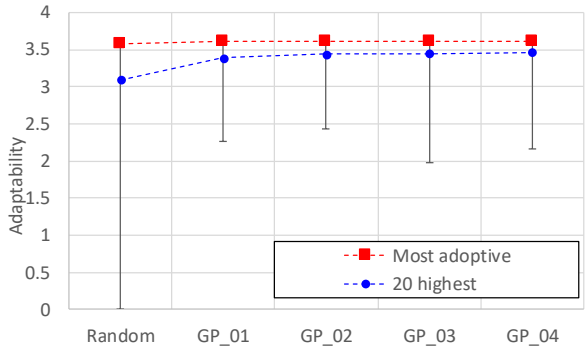

Figure 7. Change of Adaptively

BLUE: Random / Green: GP01
Red: GP02 / Cyan: GP03 / Magenta: GP04

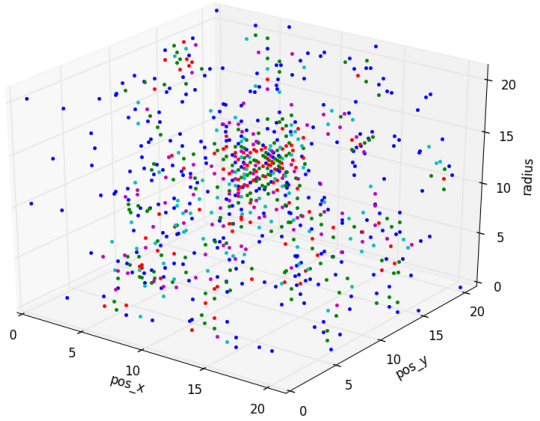

Figure 8. Analysis cases created at each stage

We repeated these five steps four times to confirm the progress of optimal analysis cases with respect to adaptively (Figure 7). The figure 8 shows the results of the random search conducted initially and the GP searches conducted at each stage. The cases found to have the highest degrees of adaptively among those searched to the given stage are shown in red, and the range of adaptively found in each stage is shown by the black line. The analyses revealed that the case with the highest degree of adaptively could be found through the initial GP search. Figure 8 is a color-coded scatter plot of analysis cases created at each stage for three-dimensional search areas of radius and the center positions of SMGA. The blue points represent the initial random search, and are plotted throughout the entire area. In contrast, points from all other stages are concentrated in specific areas. We analyzed 700 cases, which is less than 10% of the total of 9,000 analysis cases that would have to be analyzed through brute force. GP enabled us to conduct an efficient search, and for high-Adaptively areas yielded virtually the same search results as the brute-force approach; this method resulted in convergence at an earlier stage. This demonstrates the excellent applicability of GP.

ANALYSIS MODEL OF SMGA

The analytical model we derived from the process described previously was the SMGA model that most closely simulated observational data, and we used it to examine SMGA distribution and the results of response analysis.

SMGA Distribution

Figure 9 shows the SMGA distributions of the 20 highest-conforming models derived from the process described previously. These distributions are generally the same size and located in the same areas across all 20 cases. The highest-conforming case featured an SMGA radius of 2.7 km and an area of 22.9 km^2; the average radius for the 20 cases was 2.8 km, and the average area was 24.7 km^2. SMGA accounted for roughly 10% of total fault plane area, which is smaller than that of the "recipe" of Irikura et al 2003. It is also smaller than the 70km^2 area found by Ikeda et al. in the hypocenter model they created using the empirical Green's function method. However, the Ikeda et al. model assumed that SMGA release all seismic vibrations, and accordingly set the stress drop for background areas to zero. The Ikeda et al. SMGA model envelops our model; as a fault model derived from a completely different analytical method, it can produce relatively similar results.

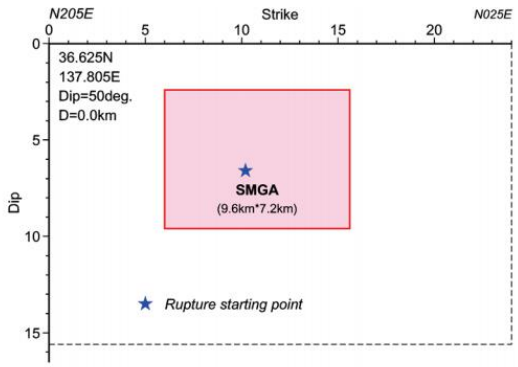

Figure 9. SMGA model of Ikeda et al. 2016

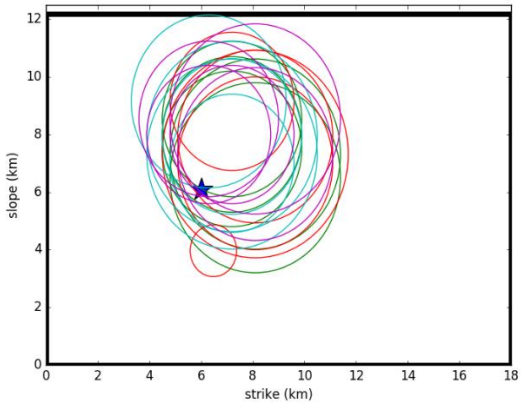

Figure 10. SMGA distribution of the 20 highest conforming models

Response Displacement Time histories

The displacement time histories for NS, EW and UD show overlapping results using SMGA (from the top 20 cases) obtained from the searches we conducted for this research in light of the results of observational data and cases where fault structure was made uniform. Modeling SMGA substantially changed displacement for the EW and UD directions, and produced results similar to observational data. We did not observe significant differences in the NS direction. However, investigations from past years have shown that the balance between displacement in the EW and UD directions changes with respect to a fault's initial stress direction. We used the results of hypocenter inversion and the like as a reference for setting the rake angle for this investigation to 60°, but the rake angle should be discussed during deliberations. If we focus on the timing of the appearance of the displacements, we can see that displacements begin to appear slightly later than in the homogeneous fault model. The timing of the appearance of displacements in the UD direction does not change much; thus, we believe the difference originates from the timing of the appearance of displacements in each direction in the SMGA model. We were able to confirm large differences in the displacement time histories from observational data, and although the results of our analysis cannot fully explain the observational data, their ability to explain the observational data in qualitative terms has improved.

Fault Rupture Timing

Figure 12 contains a contour plot of the timing of fault rupture from the analytical model that used the highest-conforming SMGA conditions. The figure also contains a contour plot that shows the results for the homogeneous fault model. In the homogeneous model, the fault ruptures outward from the hypocenter in concentric circles. Our heterogeneous model shows variance in the timing of fault ruptures.

This is likely because we set high rupture strength values to reflect high stress drop values in SMGA, and this makes it more difficult for ruptures to occur. We believe that this is a factor in the difference in timing of the appearance of displacement by direction as explained in Section 4.2.

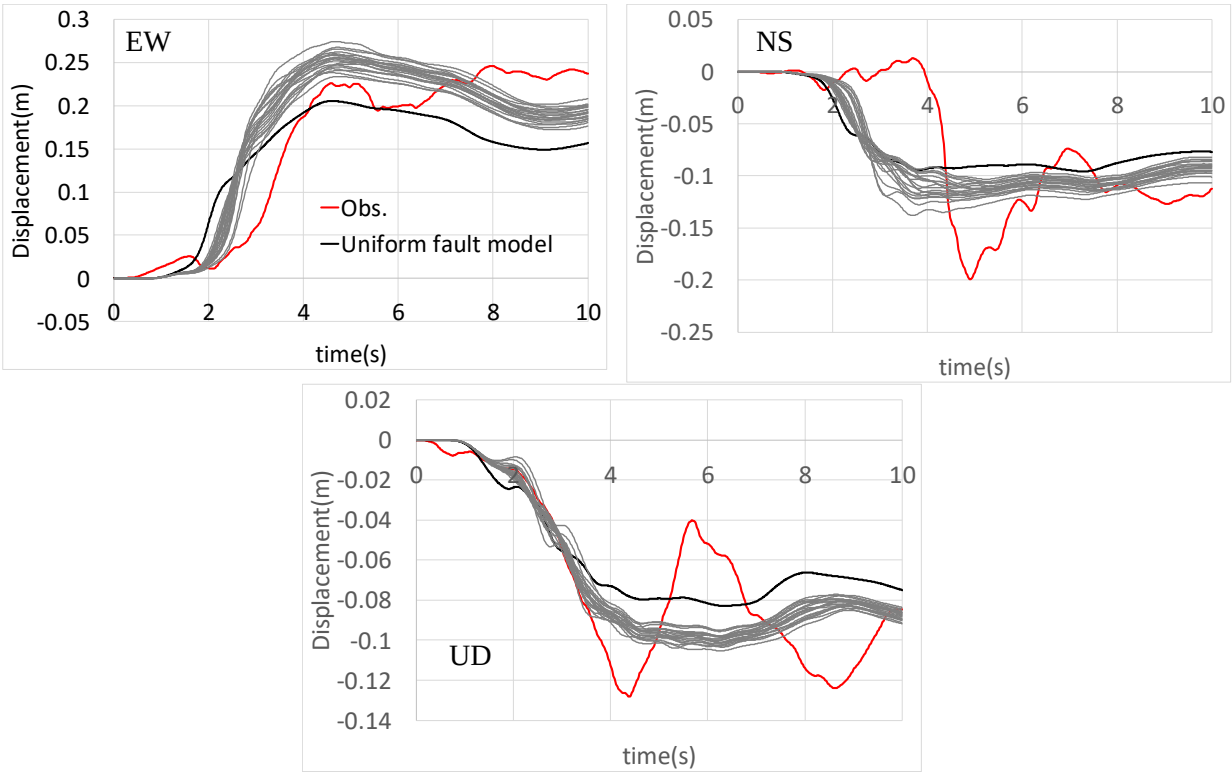

Figure 11. Response displacement time history

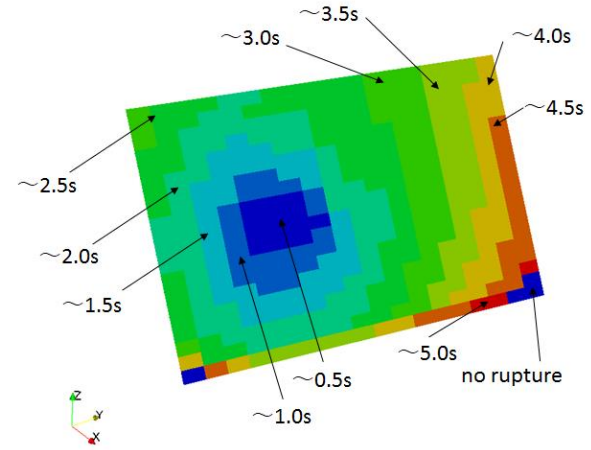

Figure 12. Contour plot of the rupture time (SMGA model)

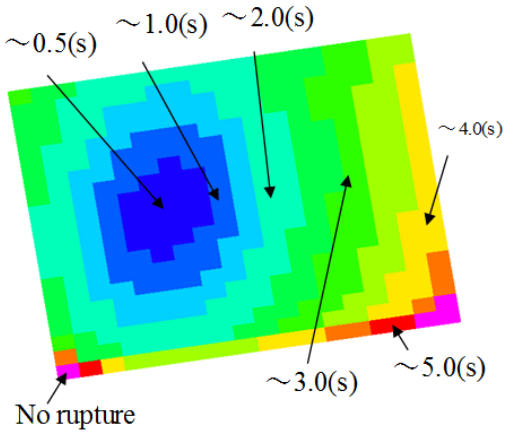

Figure 13. Contour plot of rupture time (uniformal fault model)

Slippage Contour Plot

Figure 13 is a contour plot of the amount of fault displacement at the end of the simulation. Although the amount is not substantial, the SMGA model allows us to confirm an imbalance. The maximum amount

of deformation of the ground surface plane was a particularly impressive result. This was ultimately because we positioned SMGA in areas close to the ground surface plane.

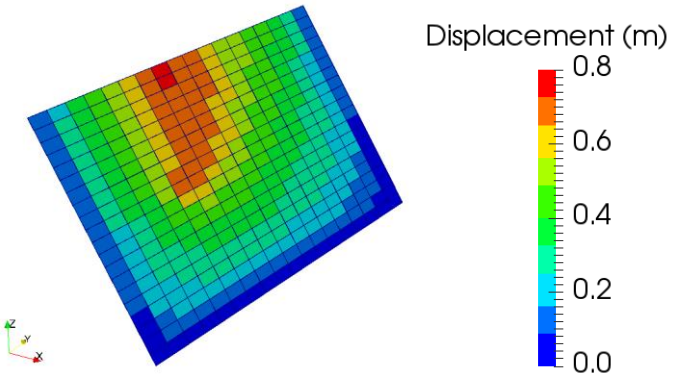

Figure 14. Contour plot of fault displacement

CONCLUSION

We used FEM to conduct dynamic fault simulations of the Kamishiro Fault Earthquake that struck Nagano Prefecture. We used Bayesian optimization to search for a model SMGA that matched the displacement time histories in observational data. The closest-matching SMGA model qualitatively matched the SMGA model of Ikeda et al. derived from a different method.

As for the response displacement time histories, modeling SMGA highlighted the trend of the matching of differences in the timing of the appearance of displacements in each direction and the like. We think that this is due to the variance in the timing of fault ruptures shown in our model, which takes fault heterogeneity into account.

In the future, we intend to conduct investigations with more parameters, and analysis that accounts for structures that straddle faults.

Acknowledgment: We would like to express our gratitude to the National Research Institute for Earth Science and Disaster Resilience for allowing us to use their K-net strong motion records as seismological observation records for this research.

NOMENCLATURE

μ	shear modulus	Δu	fault displacement
M_0	Seismic Moment	M_w	Moment magnitude
$\Delta\sigma$	Stress drop	τ_y	Yield stress

REFERENCES

David M. Boore, Christopher D. Stephens, William B. Joyner: Comments on Baseline Correction of Digital Strong-Motion Data: Examples from the 1999 Hector Mine, California, Earthquake, Bulletin of Seismological Society of America, Vol.92, No.4, pp1543-1560, 2002.

D.J.Andrews, Rupture velocity of plane strain shear cracks, Journal of Geophysical Research, Vol.81, pp.5679-5687, 1976.

Earthquake Research Committee, Headquarters for Earthquake Research Promotion, Strong motion forecasting method of the earthquake which specified an earthquake source fault (Recipe), Revision on 21/12/2009(In Japanese).

FrontISTR Workshop HP: http://www.multi.k.u-tokyo.ac.jp/FrontISTR/, Browse on 29/3/2017(In Japanese).

Goodman, R.E., Methods of geological engineering in discontinuous rocks, West Publishing Company, Ch. 8, pp. 300-368, 1976.

Hiroyuki Goto, Sumio Sawada, Ambiguity of Estimation Parameters and Noise Analysis for Dynamic Source Inversion Method Based on Walsh Functions, Journal of applied mechanics, JSCE, Vol. 9 (2006) P 745-752(In Japanese).

Japan Association for Earthquake Engineering: Report about the Earthquake at the Nagano Prefecture north in 2014, 2015(In Japanese).

Japan Nuclear Safety Institute On-site Fault Assessment Method Review Committee, Assessment Methods for Nuclear Power Plant against Fault Displacement, September 2013(Rev. Apr. 2014).

Kazuo Dan, Manami Muto, Haruhiko Shimada, Yasuhiro Ohashi, Yuko Kase, Basic examination on consecutive fault rupturing by dynamic rupture simulation, Annual Report on Active Fault and Paleoearthquake Researches, No.7, 259-271, 2007(In Japanese).

Kiyoshi Irie, Kazuo Dan, Shinya Ikutama, Kojiro Irikura, Modeling pf dynamic fault rupturing constrained by empirical relations among fault parameters of surface and subsurface faults – Toward improvement of kinematic fault model for predicting strong ground motion - , Journal of Structural and Construction Engineering, Architectural Institute of Japan, Vol. 75 (2010) No. 657 P 1965-1974(In Japanese).

Kojiro IRIKURA, Hiroe MIYAKE, Tomotaka IWATA, Katsuhiro KAMAE, Hidenori, KAWABE, Luis Angel DALGUER, Recipe for Predicting Strong Ground Motion from Future Large Earthquake, Annuals of Disas. Prev. Res. Inst., Kyoto Univ., No.46 B, 2003(In Japanese).

National Research Institute for Earth Science and Disaster Prevention: Strong-motion Seismograph Networks, http://www.kyoshin.bosai.go.jp/, Brows on 01/08/2015.

National Institute of Advanced Industrial Science and Technology: Active fault database, https://gbank.gsj.jp/activefault/index_gmap.html, Brows on 01/08/2015(In Japanese).

Rasmussen, C. E., Williams, C. K. I., Gaussian Processes for Machine Learning, The MIT Press, 2006.

S. Peyrat, K. B. Olsen, Nonlinear dynamic rupture inversion of the 2000 Western Tottori, Japan, earthquake, Geophesical Research Letters, Vol.31, L05604, 2004.

Takaaki Ikeda, Kazuo Konagai, Katsuhiro Kamae, Takashi Sato, Yuya Takase, Damage investigation and source characterization of the 2014 northern part of Nagano prefecture earthquake, Journal of JSCE(A1), Vol. 72 (2016), No. 4, p. I_975-I_983(In Japanese).

Takayuki Mizumoto, Toshihiro Tsuboi, Fusanori Miura, Fundamental study on fault rupture process and earthquake motions on and near a fault by 3D-FEM, Journal of JSCE, No.780, I-70, 27-40, 2005.1(In Japanese).

Takayuki Mizumoto, Fusanori Miura, Toshihiro Tsuboi, The fault motion simulation of 2000 Western Tottori Earthquake using 3D FEM, JSCE journal of Earthquake Engineering, August 2001(In Japanese).

Yuta MITSUHASHI, Gaku HASHIMOTO, Hiroshi OKUDA, Fujio UCHIYAMA, Fault Displacement Simula-tion Analysis of the Kamishiro Fault Earthquake in Nagano Prefecture Using the Parallel Finite Element Method, Model Design and Simulation Analysis, Communications in Computer and Information Science 603, p102-109, 2016.

Yuta MITSUHASHI, Gaku HASHIMOTO, Hiroshi OKUDA, Finite Element Modeling for Geotechnical Analysis (Extended Goodman's Joint Element and Mesh Generation Method), Paper No. 20160022, pp. 1-10, 2016(In Japanese).